

This discussion paper is/has been under review for the journal Atmospheric Chemistry and Physics (ACP). Please refer to the corresponding final paper in ACP if available.

The influence of eruption season on the global aerosol evolution and radiative impact of tropical volcanic eruptions

M. Toohey^{1,*}, K. Krüger¹, U. Niemeier², and C. Timmreck²

¹Leibniz Institute of Marine Sciences (IFM-GEOMAR), Kiel, Germany

²Max Planck Institute for Meteorology (MPI-M), Hamburg, Germany

*Invited contribution by M. Toohey, recipient of the EGU Outstanding Student Poster Award 2010

Received: 21 June 2011 – Accepted: 2 August 2011 – Published: 8 August 2011

Correspondence to: M. Toohey (mtoohey@ifm-geomar.de)

Published by Copernicus Publications on behalf of the European Geosciences Union.

ACPD

11, 22443–22481, 2011

Influence of season on impact of tropical eruptions

M. Toohey et al.

Title Page

Abstract

Introduction

Conclusions

References

Tables

Figures

◀

▶

◀

▶

Back

Close

Full Screen / Esc

Printer-friendly Version

Interactive Discussion



Abstract

5 Simulations of tropical volcanic eruptions using a general circulation model with coupled aerosol microphysics are used to assess the influence of season of eruption on the aerosol evolution and radiative impacts at the Earth's surface. This analysis is presented for eruptions with SO₂ injection magnitudes of 17 and 700 Tg, the former consistent with estimates of the 1991 Mt. Pinatubo eruption, the later a near-“super eruption”. For each eruption magnitude, simulations are performed with eruptions at 15° N, at four equally spaced times of year, and sensitivity to eruption season is quantified as the difference between the maximum and minimum cumulative anomalies.

10 Eruption season has a significant influence on aerosol optical depth (AOD) and clear-sky shortwave (SW) radiative flux anomalies for both eruption magnitudes. The sensitivity to eruption season for both fields is generally weak in the tropics, but increases in the mid- and high latitudes, reaching maximum values of ~80 %. Global mean AOD and clear-sky SW anomalies show sensitivity to eruption season on the order of 15–
15 20 %, which results from differences in aerosol effective radius for the different eruption seasons. Smallest aerosol size and largest cumulative impact result from a January eruption for the Pinatubo-magnitude, and from a July eruption for the near-super eruption. In contrast to AOD and clear-sky SW anomalies, all-sky SW anomalies are found to be insensitive to season of eruption for the Pinatubo-magnitude eruption experiment,
20 due to the reflection of solar radiation by clouds in the mid- to high latitudes. However, differences in all-sky SW anomalies between eruptions in different seasons are significant for the larger eruption magnitude, and the ~15 % sensitivity to eruption season of the global mean all-sky SW anomalies is comparable to the sensitivity of global mean AOD and clear-sky SW anomalies. Our estimates of sensitivity to eruption season are
25 larger than previously reported estimates: implications regarding volcanic AOD time-series reconstructions and their use in climate models are discussed.

Influence of season on impact of tropical eruptions

M. Toohey et al.

Title Page

Abstract

Introduction

Conclusions

References

Tables

Figures



Back

Close

Full Screen / Esc

Printer-friendly Version

Interactive Discussion



1 Introduction

Volcanic sulfate aerosols resulting from the injection of sulfur into the stratosphere by explosive volcanic eruptions can have a significant impact on the global Earth system. These aerosols reflect solar visible radiation, causing cooling at the Earth's surface, and absorb solar near-infrared and terrestrial infrared radiation, causing warming of the stratosphere (e.g., Robock, 2000).

Volcanic eruptions in the tropics have stronger climate impacts than comparable eruptions at mid- or high-latitudes, since the large-scale circulation pattern of the stratosphere, or Brewer-Dobson circulation (BDC) leads to longer stratospheric lifetimes and the possibility of global coverage for volcanic aerosols introduced into the tropical stratosphere (Hamill et al., 1997). The Brewer-Dobson circulation is generally characterized by upward motion in the tropics, poleward motion and mixing in the midlatitudes, and downward motion at polar latitudes (e.g., Holton et al., 1995). This circulation is driven by the breaking of planetary-scale Rossby waves in the midlatitude stratosphere (McIntyre and Palmer, 1983), which occurs predominantly in the winter hemisphere since these waves cannot propagate upward through the easterly winds of the summer hemisphere (Charney and Drazin, 1961). As a result, transport out of the tropical stratosphere (Vaugh, 1996), poleward meridional mass transport (Rosenlof, 1995) and two-way mixing in the midlatitudes occurs most strongly in the winter hemisphere, resulting in a seasonal cycle in the BDC.

Post-eruption aerosol evolution (at least in terms of the spatial distribution of the aerosol cloud), is largely controlled by atmospheric transport, and is thus a function of the specific meteorological conditions at the time of eruption. However, some level of explanation of aerosol evolution can be taken from the mean seasonal cycle of the BDC. Knowledge of the seasonal cycle of the BDC and related aerosol transport has been used to reconstruct volcanic forcing data sets from historical records for use in climate reconstruction modeling. For example, Ammann et al. (2003) introduced a latitudinally varying, monthly mean AOD reconstruction using a simple scheme with

Influence of season on impact of tropical eruptions

M. Toohey et al.

Title Page

Abstract

Introduction

Conclusions

References

Tables

Figures



Back

Close

Full Screen / Esc

Printer-friendly Version

Interactive Discussion



**Influence of season
on impact of tropical
eruptions**

M. Toohey et al.

Title Page

Abstract

Introduction

Conclusions

References

Tables

Figures

◀

▶

◀

▶

Back

Close

Full Screen / Esc

Printer-friendly Version

Interactive Discussion



parameterized seasonally varying stratospheric meridional aerosol transport and removal. Such a reconstruction should serve as a more realistic input in climate models than, for example, a global or hemispheric mean timeseries. Gao et al. (2008) used a similar transport and removal scheme to produce a latitudinally varying volcanic forcing data set based on ice core sulfate records which covers the last 1500 yr. Since the seasons of eruption for most of the volcanic events over this time period are unknown, Gao et al. (2008) quantified the impact of an unknown season of eruption on their reconstruction method. Using the parameterized transport scheme, they found only very small differences (maximum 3%) between the time-averaged aerosol burdens for Tabora-like eruptions in different seasons, although they also noted that general circulation model (GCM) studies would be necessary to test the detailed radiative, and dynamic responses associated with eruptions in different seasons.

Kravitz and Robock (2011) have performed simulations of volcanic aerosol evolution from high latitude Northern Hemispheric eruptions, and found that season of eruption is important in determining the radiative impact due to the seasonal variation in solar insolation at high latitudes, and seasonal variations in the rate of removal of aerosols from the high latitude stratosphere. The simulations described by Kravitz and Robock (2011) were of eruptions of 1.5–5 Tg SO₂ injection, and were performed using prescribed aerosol effective radius.

This work aims to quantify the influence of eruption season on the impact of tropical volcanic eruptions using a detailed GCM with coupled aerosol microphysics. Specifically, we aim to address the following questions:

1. How does season of eruption influence the resulting aerosol optical depth, in terms of its global mean and zonal mean evolution?
2. How does season of eruption impact the resulting anomalies in solar shortwave (SW) radiative flux at the surface, and is the sensitivity of surface SW radiative flux to eruption season the same as that for AOD?

**Influence of season
on impact of tropical
eruptions**

M. Toohey et al.

[Title Page](#)[Abstract](#)[Introduction](#)[Conclusions](#)[References](#)[Tables](#)[Figures](#)[⏪](#)[⏩](#)[◀](#)[▶](#)[Back](#)[Close](#)[Full Screen / Esc](#)[Printer-friendly Version](#)[Interactive Discussion](#)

3. How does the sensitivity to eruption season of AOD and SW anomalies change for eruptions of different stratospheric sulfur injection magnitudes?

In order to address these questions, we have performed ensemble simulations for eruptions on the first day of January, April, July, and October, for eruptions of two magnitudes, with stratospheric SO₂ injections of 17 and 700 Tg. The smaller injection magnitude is consistent with estimates of the June 1991 Mt. Pinatubo eruption (Guo, 2004a). Our simulations of this magnitude eruption thus can be considered as roughly addressing the question of how the impact of Pinatubo might have changed had it erupted in a different time of year. The larger injection magnitude is roughly 40 times that of Pinatubo, and is nearly as large as the approximately-defined 800 Tg lower limit for SO₂ injection by a “super-eruption” (Self, 2006). Examining such a large eruption magnitude allows us to explore how global aerosol transport, and its dependence on season, changes for eruptions where aerosol heating significantly perturbs stratospheric dynamics.

The paper is organized as follows: Sect. 2 describes the model and the simulations used in this study. Section 3 contains a comparison of observations of perturbed conditions resulting from the 1991 Pinatubo eruption with Pinatubo-magnitude eruption simulations, and tests the impact of eruption longitude on the model simulations. In Sect. 4, we quantify the sensitivity of the model simulated aerosol optical depth and surface radiative anomalies to season of eruption for the two eruption magnitudes introduced above. Conclusions are given in Sect. 5.

2 Method

2.1 Model description

The study was performed using the coupled aerosol-GCM MAECHAM5-HAM (Niemeier et al., 2009). MAECHAM5 (Giorgetta et al., 2006) is a middle atmosphere version of the

ECHAM5 GCM (Roeckner et al., 2003). The model solves prognostic equations for vorticity, divergence, surface pressure and temperature, expressed in terms of spherical harmonics with a triangular truncation. Trace components, including SO₂ and aerosols, are transported with a flux form semi-Lagrangian transport scheme (Lin and Rood, 1996). ECHAM5 radiation is based on the six band (1.85–4 μm) SW radiative transfer scheme of Fouquart and Bonnel (1980), and the RRTM (Rapid Radiative Transfer Model) 16 band (3.3–100 μm) longwave radiation scheme (Mlawer et al., 1997). It considers the absorption of greenhouse gases as well as scattering and absorption by clouds and aerosols. For the radiation calculations concerning volcanic aerosols, optical parameters are calculated online from the time dependent aerosol mass mixing ratio and normalized optical parameters (extinction, absorption coefficients, and asymmetry factor).

MAECHAM5 is used here in a free-running climate mode, with T42 spectral truncation and 39 vertical levels up to 0.01 hPa. At this model resolution, the model has no quasi-biennial oscillation (QBO): in control simulations, equatorial stratospheric winds are easterly throughout the year. Sea surface temperatures are prescribed as an annually repeating climatology.

Model processes related to sulfate aerosols are calculated by the aerosol microphysical module HAM (Stier et al., 2005), which is interactively coupled to MAECHAM5. HAM has been adopted for stratospheric conditions (as well as for high SO₂ concentrations) as outlined by Niemeier et al. (2009). Changes to M7, the microphysical core of HAM (Vignati, 2004), were performed according to boxmodel studies for large volcanic eruptions (Kokkola et al., 2009). Volcanic simulations with the MAECHAM5-HAM model are initiated by injecting SO₂ directly into the lower stratosphere into a model gridbox corresponding to the volcano's geographical location, and the model layer corresponding to the pressure height level of 30 hPa (~24 km). This height is chosen so as to be roughly consistent with estimates of the height of SO₂ injection by the Pinatubo eruption (Read et al., 1993; Guo, 2004b). The model then simulates the full lifecycle of the volcanic aerosols, including oxidation of SO₂ to H₂SO₄; aerosol formation and

Influence of season on impact of tropical eruptions

M. Toohey et al.

[Title Page](#)[Abstract](#)[Introduction](#)[Conclusions](#)[References](#)[Tables](#)[Figures](#)[◀](#)[▶](#)[◀](#)[▶](#)[Back](#)[Close](#)[Full Screen / Esc](#)[Printer-friendly Version](#)[Interactive Discussion](#)

growth via nucleation, condensation, accumulation and coagulation; vertical redistribution via sedimentation; and finally the removal processes wet and dry deposition. The full coupling of the HAM module with MAECHAM5 allows for feedbacks, whereby the absorption of outgoing longwave radiation by aerosols, and the associated local heating of the atmosphere, leads to anomalous atmospheric dynamics. Through such feedbacks, the transport of volcanic aerosols can be significantly different than that of a passive tracer (e.g., Young et al., 1994; Timmreck et al., 1999).

2.2 Model experiments

We focus here on comparing results from simulations of eruptions of two magnitudes. The magnitude of our larger SO₂ injection (700 Tg) is derived from the erupted masses (Kutterolf et al., 2008a,b) and petrological-method-derived SO₂ emission estimates (Metzner et al., 2011) of the “Los Chocoyos tephra” from the 84 ka B.P. eruption at the present-day site of the Atitlan caldera in Guatemala (Rose et al., 1987). Simulations of the Los Chocoyos eruption were performed by injecting 700 Mt of SO₂ in the model gridbox closest to 14.6° N, 91.2°W. We also perform simulations of a hypothetical eruption at the same location with an SO₂ injection based on estimates of the 1991 Mt. Pinatubo eruption. This SO₂ injection and location also correspond roughly to estimates for the “E-Fall” eruption of 51 ka B.P. (Metzner et al., 2011). The latitude of the simulated eruptions is also consistent with the peak of the latitudinal distribution of active volcanoes (Schmincke, 2004). For both eruption magnitudes, we perform simulations with eruptions on the first day of January, April, July and October. Each simulation was run for four years after the eruption. This time period contains the vast majority of the atmospheric response to volcanic aerosols; in the model simulations, stratospheric aerosol loading is found to have decreased to less than 2% of maximum loading after 4 yr for both eruption magnitudes. In the following, we refer to the two sets of eruption simulations for different eruption seasons as the E700 and E17 experiments, for the 700 and 17 Tg SO₂ injections, respectively. For each season of eruption, we perform multiple model integrations ($n = 6$ for E700, $n = 12$ for E17), where for each

Influence of season on impact of tropical eruptions

M. Toohey et al.

Title Page

Abstract

Introduction

Conclusions

References

Tables

Figures

◀

▶

◀

▶

Back

Close

Full Screen / Esc

Printer-friendly Version

Interactive Discussion



integration, the eruption branches from a different year of a 20 yr control run. More ensemble members were performed for the smaller eruption magnitude in order to improve the statistical significance of the smaller ensemble mean anomalies. All results shown are full ensemble means for each magnitude and eruption month. Anomalies are calculated as the difference between experiment runs and the 20 yr control run.

Lastly, in order to better compare with observations of the Pinatubo aerosol evolution, and assess the importance of eruption longitude, we have performed simulations with eruptions on 15 June, at the approximate locations of the Los Chocoyos and Pinatubo eruptions. These results are used only in Sect. 3.

3 Model validation: Pinatubo comparisons

Results of a prior MAECHAM5-HAM simulation of the 15 June 1991 Pinatubo eruption were compared to observations by Niemeier et al. (2009). They found that simulated zonal mean, monthly mean AOD showed reasonably good agreement with AVHRR and SAGE II satellite observations with respect to the timing and location of peak values, even though the simulations are performed in climatological mode. Quantitatively, peak AOD values from the model were 10–20 % higher than peak values observed by AVHRR, and larger by an even larger factor than SAGE II observations, although SAGE II measurements are highly uncertain in the months immediately after the Pinatubo eruption due to saturation effects (Russell et al., 1996).

Here we compare observations of the impacts of the Pinatubo eruption with new MAECHAM5-HAM simulations of Pinatubo-magnitude eruptions at two different longitudes, in order to test whether the longitude of the eruption site plays any role in the volcanic impacts. The model latitude of the eruption in the two experiments (15.3° N) is the closest model latitude to that of both the Pinatubo (15.1° N) and the Los Chocoyos (14.6° N) eruption sites. The two longitudes used correspond to the closest model longitudes to those of the Pinatubo (120.3° E), and Los Chocoyos eruption (91.2° W).

Influence of season on impact of tropical eruptions

M. Toohey et al.

Title Page

Abstract

Introduction

Conclusions

References

Tables

Figures

◀

▶

◀

▶

Back

Close

Full Screen / Esc

Printer-friendly Version

Interactive Discussion



**Influence of season
on impact of tropical
eruptions**

M. Toohey et al.

[Title Page](#)[Abstract](#)[Introduction](#)[Conclusions](#)[References](#)[Tables](#)[Figures](#)[⏪](#)[⏩](#)[◀](#)[▶](#)[Back](#)[Close](#)[Full Screen / Esc](#)[Printer-friendly Version](#)[Interactive Discussion](#)

Figure 1 shows zonal mean mid-visible ($0.55\ \mu\text{m}$) volcanic aerosol optical depth (AOD) at labeled latitude bands from an ensemble of Pinatubo-magnitude eruption simulations compared to the those from the Sato et al. (1993) AOD timeseries, based in this time period on measurements from the SAGE II satellite instrument. As in Niemeier et al. (2009), the model AOD is notably larger than the observations in the months immediately following the eruption. AVHRR retrievals (not shown here) have an AOD maximum in the tropics of approximately 0.3, in closer agreement with the AOD of the model. In the tropics, the model AOD falls below the Sato et al. (1993) AOD after approximately 6 months, and the decay of AOD in the tropics is faster in the model than observed. In the extratropics, while the magnitude of the model peak AOD is again larger than that of the observations, the timing of the peaks is quite consistent with the observations. The seasonality of the AOD evolution is also quite consistent between model and observations: note for example the double-peak at 35°S at approximately 5 and 12 months after the eruption, and the periodic flattening of the AOD decay at 35°N between 12 and 18 months, and 24 and 30 months. The decay in AOD at the high latitudes is faster in the model than in observations, especially in the SH. Niemeier et al. (2009) found the model aerosol effective radius to be consistent with midlatitude lidar measurements, albeit at the upper limit of those measurements, and suggested a slight high-bias in the model effective radius might lead to larger sedimentation rates, explaining the faster decay of AOD in the model.

Figure 2 shows top-of-atmosphere (TOA) (SW) radiative flux anomalies from the model simulations compared to observations by the Earth Radiation Budget Experiment (ERBE) (Barkstrom; Barkstrom and Smith, 1986). We have used Edition 3 Rev 1 data set from the Earth Radiation Budget Satellite (ERBS) Nonscanner Wide Field of View, which have been corrected for a change in satellite altitude and instrument drift during the measurement period, and agree well with other satellite-based earth radiation budget records (Wong et al., 2006). Since monthly means have been found to create a spurious semi-annual cycle in the data, 36-day averages are used (Wielicki et al., 2002) in the tropical data set, and 72-day means in the near-global data set. ERBE

TOA SW anomalies are calculated with respect to the 1985–1989 mean, while model anomalies are calculated with respect to a 20 yr control simulation. MAECHAM5-HAM simulated TOA SW flux anomalies show excellent agreement with the ERBE observations, in both tropical and near-global mean.

5 The fact that model TOA SW flux anomalies agree well with ERBE suggests the discrepancy between model and observed AOD immediately following the eruption may be more a function of underestimated observations rather than an overestimate by the model. After the initial post-eruption period, discrepancies between model and observed AODs suggest the model overestimates the transport of aerosol to high latitudes, and has a faster removal rate. Nonetheless, the qualitative features of aerosol transport in the model agree reasonably well with observations, including the timing of peak AOD levels, and seasonal variations in AOD decay rate.

10 Simulations of Pinatubo-strength eruptions at two different longitudes showed no systematic bias in AOD evolution or radiative impact in our MAECHAM5-HAM runs. This result increases confidence that the results of the next section can be regarded as generally applicable to eruptions at a particular tropical latitude, independent of longitude.

4 Sensitivity experiments

15 Here we investigate the aerosol transport and short-wave radiative impacts of simulated tropical eruptions, and the sensitivity of these impacts to eruption season. The radiative effects of volcanic aerosols are complex, as are definitions of “radiative forcing” used in volcanic studies and more general literature (see, e.g., discussion in Stenchikov et al., 1998). Since the primary climatic impact of volcanic aerosols is the reflection of solar SW radiation, which decreases the SW radiative flux at the Earth’s surface, and hence the energy input to the Earth system, we focus here on anomalies in SW surface fluxes with respect to climatological values from a control run. In addition to surface flux anomalies, we have also examined top-of-atmosphere SW flux anomalies, but

Influence of season on impact of tropical eruptions

M. Toohey et al.

Title Page

Abstract

Introduction

Conclusions

References

Tables

Figures



Back

Close

Full Screen / Esc

Printer-friendly Version

Interactive Discussion



since the results are very similar, only the results of our analysis of surface fields will be shown here. However, as will be shown, sensitivity to eruption season is somewhat different for clear-sky and all-sky SW, therefore both fields will be considered. In addition, we also consider the mid-visible (0.55 μm) volcanic aerosol optical depth (AOD), also calculated as the anomaly in AOD between the volcanically perturbed simulations and a control run. Each of these fields will be considered in terms of zonal and global means. Two eruption magnitudes are investigated, and are discussed separately in the following two subsections.

4.1 E17: Pinatubo-magnitude experiment

Through inspection of the zonal mean AOD evolution for the E17 experiment (Fig. 3a), it is clear the season of eruption plays a significant role in the timing and strength of volcanic aerosol transport out of the tropics into the extratropics. The qualitative features of the AOD distributions of Fig. 3 can be explained in terms of the seasonal variation of the BDC, with, for example, stronger aerosol transport to the NH after eruptions in NH fall (Oct) and winter (Jan) leading to larger AOD values in the NH. The transport of aerosols is not symmetric with respect to hemisphere and season for this eruption magnitude and location, i.e., the transport to the SH midlatitudes for a SH winter eruption is much weaker than to the NH midlatitudes for a NH winter eruption. It appears the latitude of the eruption, on the northern edge of the tropics, plays a significant role in producing this hemispheric bias in AOD distribution.

Clear-sky surface SW anomalies are given in Fig. 3b. These absolute anomalies are a function of both the spatio-temporal evolution of the volcanic AOD, and the seasonally varying solar insolation pattern (also shown in Fig. 3a). As a result, clear-sky SW anomalies do not exactly follow the AOD patterns: for example, 6–9 months after an April eruption the AOD pattern is reasonably hemispherically symmetric, while the clear-sky SW anomalies are much stronger in the SH, owing to the fact that this time period coincides with SH summer when the local solar insolation is at a maximum. Note also that the AOD maximum at high NH latitudes for a January eruption coincides

Influence of season on impact of tropical eruptions

M. Toohey et al.

Title Page

Abstract

Introduction

Conclusions

References

Tables

Figures

◀

▶

◀

▶

Back

Close

Full Screen / Esc

Printer-friendly Version

Interactive Discussion



exactly with maximum solar insolation, leading to quite strong clear-sky SW anomalies.

All-sky surface shortwave anomalies are shown in Fig. 3c. These anomalies are a function of the clear-sky SW anomalies and the degree of cloudiness in the model. The climatological ratio of all-sky to clear-sky SW from the control run is given in Fig. 4.

Maximum cloudiness (hence lowest all-sky to clear-sky ratio) is found in the mid- to high latitudes, which explains the reduction in the relative amplitude of the all-sky SW anomalies in the high latitudes compared to in the tropics. Clouds add a large degree of noise to the all-sky SW anomaly field: the standard deviation of the all-sky SW anomaly field from the climatology is shown in Fig. 4. The ensemble mean all-sky SW anomalies shown in Fig. 3c, with maximum magnitudes of $5\text{--}10\text{ W m}^{-2}$, are roughly comparable to the standard deviation of all-sky SW in the control run. This means that while the all-sky SW anomalies in Fig. 3c are significant in the ensemble mean, they are of the same magnitude as the natural variability of the model all-sky SW field.

Quantifying the influence of eruption season on the impact amounts to condensing the information in Fig. 3 into some measure of sensitivity. As a first step, we integrate the anomalies shown in Fig. 3 in time, leading to cumulative anomalies. Cumulative anomalies of SW radiation express the total change in solar energy arriving at the surface as a consequence of the volcanic eruption, and so is a good measure of the total radiative impact. A cumulative anomaly is a robust measure of the impact (compared to, e.g., a time average), since, in theory, it should not matter over what time period one integrates over since the volcanic anomalies decay to zero after a few years. We calculate cumulative AOD and SW anomalies by summing the respective field over two years, and are presented in units of months (for the unitless AOD) and $\text{W m}^{-2}\cdot\text{months}$ for SW anomalies. It should be noted that cumulative SW anomalies as calculated here are a measure of energy per unit area, and can easily be scaled to units of J m^{-2} , but are shown here in $\text{W m}^{-2}\cdot\text{months}$ both for consistency with the cumulative unit of AOD, and for easier comparison with the raw anomalies of Fig. 3.

Figure 5 shows cumulative AOD, clear-sky SW and all-sky SW anomalies in terms of zonal and global means. Cumulative fields for eruptions in different seasons are

Influence of season on impact of tropical eruptions

M. Toohey et al.

[Title Page](#)[Abstract](#)[Introduction](#)[Conclusions](#)[References](#)[Tables](#)[Figures](#)[Back](#)[Close](#)[Full Screen / Esc](#)[Printer-friendly Version](#)[Interactive Discussion](#)

designated by colors. The influence of season on the impact of volcanic eruptions can be quantified by comparing the magnitude of the impact for the eruption month in which the impact is greatest, to the magnitude of impact for the eruption month in which the impact is smallest. Differences between maximum and minimum response are shown by black lines for each latitude. Gray shading indicates the 95 % confidence interval of the max-to-min differences, as calculated using the student's t-test.

Examining first the cumulative AOD, we see the largest sensitivity to eruption season in the NH mid- to high-latitudes. The January eruption simulations lead to the highest AOD values from 30° S to 90° N, and south of 30° S the AOD for January eruption is only slightly lower than that for an April eruption. In the global mean, a January eruption leads to a significantly larger AOD than for the other months. We explore reasons for the larger cumulative AOD seen for a January eruption with the aid of Fig. 6. The AOD for a January eruption is larger than for other eruption months from approximately four months after the eruption onward (Fig. 6a). While the sulfate mass burden (Fig. 6b) for all eruption months are comparable for the first 6–8 months, the aerosol effective radius (Fig. 6c) is notably smaller for a January eruption. Smaller aerosols scatter SW radiation more efficiently, and also have a smaller sedimentation rate, which increases their stratospheric lifetime. Through these related mechanisms, a smaller aerosol effective radius can explain the larger January eruption AOD in the E17 experiment. The smaller effective radius for the January eruption is itself likely related to the vertical distribution of sulfate for a January eruption. Sulfate burdens for a January eruption are notably shifted to higher altitudes than for other eruption months. Figure 6d shows, for example, the sulfate burden timeseries at 10 hPa, for which the burden following the January eruption is larger than for all other eruption months. It has been shown (Niemeier et al., 2010) that the stratospheric injection height of SO₂ has an appreciable effect on aerosol size, with higher injection heights leading to smaller particles. It appears that in the experiments described here, the season of eruption has an influence on aerosol size through the seasonal cycle of tropical upwelling (e.g. Randel et al., 2002), with NH winter eruptions leading to a

Influence of season on impact of tropical eruptions

M. Toohey et al.

Title Page

Abstract

Introduction

Conclusions

References

Tables

Figures

◀

▶

◀

▶

Back

Close

Full Screen / Esc

Printer-friendly Version

Interactive Discussion



higher mean height of aerosol burden, which in turn leads to smaller aerosol particles. Thus, because of the seasonality of stratospheric dynamics, the season of eruption can influence not only the spatial evolution of volcanic aerosols, but also their size distribution and cumulative global mean AOD.

5 Cumulative clear-sky SW anomalies (Fig. 5b) show significant sensitivity to eruption season poleward of 30° in both hemispheres, and maximum absolute sensitivity between 55° and 65° of both hemispheres. Like the AOD, January clear-sky SW anomalies are larger than for the other months at most latitudes north of 30° S, and the global mean clear-sky SW anomaly for a January eruption is significantly larger than those for
10 the other eruption months.

In contrast to the AOD and clear-sky SW anomalies, cumulative all-sky SW anomalies for the different seasons of eruptions are basically indistinguishable. Differences between the eruption seasons are insignificant between approximately 60° S and 60° N.

15 In order to compare the degree of sensitivity to eruption season of the fields in Fig. 5, a percent sensitivity is shown in Fig. 7, where percent sensitivity refers to the maximum-minimum difference divided by the minimum response. A 100 % sensitivity then implies that the maximum response is twice that of the minimum response. Thick lines in Fig. 7 refer to where the sensitivity is significant at the 95 % level, i.e., where the gray confidence intervals of Fig. 5 do not include zero.

20 Percent sensitivity for AOD is minimum in the tropics, and increases towards the poles, reaching maximums of 75 % in the NH and 90 % at the south pole. Clear-sky SW percent sensitivity is smaller than that of the AOD in the tropics, but larger in the high latitudes, owing to the amplifying effect of the strong seasonal cycle in solar insolation at the high latitudes. All-sky SW sensitivity is only significant at latitudes greater than
25 60° in both hemispheres, and notably noisier than the clear-sky SW sensitivity. While the latitudinal structure of the all-sky sensitivity is somewhat consistent with the clear-sky SW and AOD sensitivity pattern, there is also some indication that the all-sky SW sensitivity is less than that of the clear-sky anomalies in the midlatitude (for example, between 30 and 60° S).

Influence of season on impact of tropical eruptions

M. Toohey et al.

Title Page

Abstract

Introduction

Conclusions

References

Tables

Figures

◀

▶

◀

▶

Back

Close

Full Screen / Esc

Printer-friendly Version

Interactive Discussion



Influence of season on impact of tropical eruptions

M. Toohey et al.

Title Page

Abstract

Introduction

Conclusions

References

Tables

Figures

◀

▶

◀

▶

Back

Close

Full Screen / Esc

Printer-friendly Version

Interactive Discussion



The sensitivity of the global mean AOD and clear-sky SW anomalies are on the order of 20 %, and are both significantly greater than zero. On the other hand, the global mean all-sky SW anomalies are greatly reduced compared to the AOD and clear-sky sensitivity, and is not significantly greater than zero. This reduction in sensitivity suggests the presence of some mechanism that reduces the sensitivity of all-sky SW anomalies compared to clear-sky SW anomalies and AOD. It has been noted (e.g., Bender et al., 2010) that climate models often produce a decrease in cloud fraction as a result of volcanic forcing. Such a negative feedback mechanism – wherein decreases in surface SW brought about by reflection of SW by volcanic aerosols are partially compensated by increases in surface SW brought about by decreases in cloud cover – could conceivably lead to a reduction in sensitivity to eruption season. A detailed analysis of cloud feedbacks is beyond the scope of this work.

4.2 E700: near-super eruption experiment

Similar to the results for E17, for E700 (Fig. 8a) there are larger AOD values in the hemispheres for which the eruption occurs in winter and fall, following the expected seasonal cycle of the BDC. For E700, the hemispheric asymmetry in AOD is relatively symmetric with respect to season, in the sense that the aerosol burden for a July eruption is roughly the mirror image of that for the January eruption.

The most striking difference in the large scale spatio-temporal morphology of the AOD between the two eruption magnitudes is the appearance of strong gradients in AOD at $\sim 60^\circ$ N and $\sim 60^\circ$ S in the E700 simulations. It was shown that absorption of infrared radiation by volcanic aerosols after the 1991 Mt. Pinatubo eruption changed the meridional temperature gradient in the stratosphere (Labitzke and McCormick, 1992), which, through the thermal wind balance, led to westerly anomalies in zonal mean zonal wind (e.g., Kodera, 1994; Perlwitz and Graf, 1995; Kirchner et al., 1999; Kodera and Kuroda, 2000a,b; Shindell et al., 2001). In the E700 simulations, anomalous heating of the tropical stratosphere leads to temperature anomalies of over 30 K (not shown here), and significant anomalies in zonal wind. Figure 9 shows the time evolution of the

volcanically induced anomalous zonal wind at 50 hPa at 60° N and 60° S, for both E17 and E700 experiments. The zonal wind anomalies for E700 are strong enough that they produce winter-like polar-vortices simultaneously in both hemispheres, lasting for more than a year after the eruption. Polar vortices act as barriers to meridional transport (Schoeberl and Hartmann, 1991), and we hypothesize that the blocking of poleward aerosol transport at the induced polar vortex enhances the local meridional gradient in aerosol burden, in turn enhancing the temperature anomaly gradient and the resulting zonal wind anomalies. This constitutes a positive feedback mechanism which can help explain the persistence of the induced polar vortices. In both hemispheres, for all seasons of eruption, wind anomalies following the E17 eruptions are insignificant compared to the natural variability, while for E700, ensemble mean zonal wind anomalies are significantly larger than the 95 % natural variability bounds for 12-18 months after the eruption. In the SH, the anomalies are almost twice as strong, with peak anomalies reaching almost 50 m/s at this latitude and height. As in the NH, the SH anomalies are significant for around 12 to 18 months after the eruption, but in contrast to the NH, the anomalies vary somewhat with local season, with peaks occurring in SH fall (characteristic of a early forming winter vortex) and in SH spring (characteristic of a long-lasting winter vortex).

Clear-sky SW anomalies, shown in Fig. 8, are a function of both the AOD and the seasonal and latitudinal variations in solar insolation. Latitude-time AOD evolution is roughly similar for the January and October eruptions, with stronger AOD in the NH midlatitudes than in the SH midlatitudes. However, the absolute SW anomalies are relatively equal between hemispheres for the October eruption, but much more asymmetric for the January eruption, with larger anomalies in the NH. This is a result of the NH peak in AOD coinciding with the NH peak in solar insolation, while the October eruption NH peak in AOD occurs roughly in the midpoint of the midlatitude solar insolation cycle.

As was the case for E17, clouds greatly reduce the volcanic impact on all-sky SW anomalies in the mid- to high-latitude regions. As a result, much of the sensitivity to

Influence of season on impact of tropical eruptions

M. Toohey et al.

[Title Page](#)[Abstract](#)[Introduction](#)[Conclusions](#)[References](#)[Tables](#)[Figures](#)[⏪](#)[⏩](#)[◀](#)[▶](#)[Back](#)[Close](#)[Full Screen / Esc](#)[Printer-friendly Version](#)[Interactive Discussion](#)

eruption season displayed by the clear-sky fields is greatly reduced in the all-sky SW field: for example the all-sky SW anomalies for January and October are much more similar than the clear-sky SW anomalies for the same months.

Figure 10 shows cumulative AOD and SW anomalies for the E700 experiment. Interestingly, for this larger eruption, both January and July eruptions lead to larger global mean AODs than April and October eruptions. Maximum cumulative AOD is produced by a July eruption, as opposed to the E17 experiment, for which January eruptions produced the maximum cumulative AOD. Examination of effective radius and aerosol burden at 10 hPa (not shown) reveals that while both January and July eruptions lead to larger aerosol burdens at high stratospheric altitudes, a July eruption produces a somewhat smaller effective radius. The latitudinal spread of the AOD following a July eruption is relatively hemispherically balanced (see Fig. 10a); it may be that this larger horizontal spread of the aerosols after a July eruption leads to smaller aerosols and a larger and longer lasting AOD. In contrast to the E17 results, AOD sensitivity to eruption season in the high latitudes is weaker than in the midlatitudes: the cumulative AODs at high latitudes are comparatively small for all months of eruption due to the blocking of poleward aerosol transport by the polar vortices.

Clear-sky SW anomalies roughly follow the AOD patterns, and show maximum sensitivity to eruption season at $\sim 50^\circ$ in both hemispheres. However, due to clouds, the absolute reduction in all-sky SW anomalies is greatly suppressed in the $40\text{--}60^\circ$ regions. In contrast to the E17 experiment, the absolute sensitivity to eruption season everywhere except the SH polar region is significantly greater than zero.

Percent sensitivities to eruption season for E700 are shown in Fig. 11. As for E17, E700 AOD sensitivity is minimum in the tropics, and increases with latitude. However, blocking of poleward transport of aerosols by the induced polar vortices leads to a weakened sensitivity at polar latitudes, resulting in maximum AOD sensitivity for E700 around $50\text{--}65^\circ$ in each hemisphere. The sensitivity of both clear-sky and all-sky SW anomalies is generally less than that of AOD, except for approximately $40\text{--}60^\circ$ S, where the interaction of the seasonal dependence of solar insolation amplifies the AOD

Influence of season on impact of tropical eruptions

M. Toohey et al.

[Title Page](#)[Abstract](#)[Introduction](#)[Conclusions](#)[References](#)[Tables](#)[Figures](#)[◀](#)[▶](#)[◀](#)[▶](#)[Back](#)[Close](#)[Full Screen / Esc](#)[Printer-friendly Version](#)[Interactive Discussion](#)

difference, and SW anomaly sensitivity reaches over 80 %.

In the E700 eruption experiment, zonal mean and global mean AOD show smaller percent sensitivity to eruption season than was the case for the E17 experiment, with global mean sensitivity of $\sim 18\%$ compared to 25% for E17. Similarly, the clear-sky SW anomaly percent sensitivity for E700 is less than that of E17. The smaller relative sensitivity to eruption season for the E700 experiment compared to E17 as calculated here is due to a combination of at least two factors. Firstly, the aerosol distribution and AODs resulting from the E700 eruptions are more hemispherically symmetric than for E17. As the aerosol geographic distribution becomes more uniform with increasing eruption magnitude, the percent sensitivity to eruption season is seen to decrease. Secondly, it should be pointed out that our estimates of sensitivity are lower limits, since we test only four eruption dates, and thus a maximum-to-minimum sensitivity calculated using a larger number of eruption dates can only be larger than our estimates. The degree to which this sampling error of our experiment underestimates the true sensitivity is related to the timescale of the impacts. Since the peak in AOD for the E700 simulations is shorter-lived than in the E17 simulations, it is likely that our analysis method underestimates the true sensitivity of the larger eruption more strongly than for the weaker eruption.

Whereas global mean all-sky anomaly sensitivity for E17 was found to be much reduced compared to AOD, and insignificant, the all-sky SW anomaly sensitivity for E700 is comparable to that of the AOD, with magnitude of $\sim 18\%$, and is significantly greater than zero. In the extratropics of both hemispheres, all-sky SW anomaly sensitivity is often greater than 50% .

5 Conclusions

In this study, MAECHAM5-HAM coupled aerosol-GCM simulations have been used to assess the influence of eruption season on the impacts of tropical eruptions. Model simulations of the 1991 Mt. Pinatubo eruption show excellent agreement with TOA SW flux measurements from the ERBE instrument, and also good agreement with Sato

Influence of season on impact of tropical eruptions

M. Toohey et al.

Title Page

Abstract

Introduction

Conclusions

References

Tables

Figures



Back

Close

Full Screen / Esc

Printer-friendly Version

Interactive Discussion



et al. (1993) AOD timeseries beginning approximately 6 months after the eruption, especially with regard to the magnitude and seasonal variation of AOD. Furthermore, it was shown that model simulations of a Pinatubo-like eruption at two different longitudes resulted in no significant differences in AOD or SW anomalies. This result implies that the results of our model sensitivity study are not strongly influenced by the choice of eruption longitude, and can be considered valid for all eruptions at similar latitude.

In the MAECHAM5-HAM coupled aerosol-GCM, season of eruption plays a significant role in the space-time evolution of the AOD. Variations in the AOD pattern are qualitatively understandable in terms of seasonal variations in the BDC of the stratosphere, characterized by stronger poleward transport and mixing in the winter hemisphere. The BDC affects the timing and strength of transport of aerosols out of the tropics into mid- and high latitudes, leading to generally larger AODs in the hemisphere experiencing winter at the time of the eruption.

The sensitivity of AOD to eruption season, quantified as the percent difference between maximum and minimum AOD, is weak in the tropics and generally increasing in strength towards the poles, with maximum sensitivity of around 90%. We find that the seasonality of the BDC can affect not just the zonal mean AOD evolution, but also the global mean AOD. We found that eruptions in certain seasons led a smaller aerosol effective radius, which produced a stronger and longer lasting AOD. We hypothesize that seasonal variations in stratospheric dynamics, including tropical upwelling and horizontal transport out of the tropics affect the growth and lifetime of stratospheric aerosol particles. As a concrete example, in simulations of a Pinatubo-like eruption, an eruption in January led to a ~25% larger global mean AOD than eruptions in other months. Future studies of the influence of stratospheric dynamics on aerosol formation and growth, especially one which would include variability related to the QBO (see, e.g., Trepte and Hitchman, 1992), could be interesting with regards to both volcanic impacts and geoengineering.

The influence of eruption season on AOD evolution is much stronger in the MAECHAM5-HAM simulations described here than was reported by Gao et al. (2008)

Influence of season on impact of tropical eruptions

M. Toohey et al.

Title Page

Abstract

Introduction

Conclusions

References

Tables

Figures



Back

Close

Full Screen / Esc

Printer-friendly Version

Interactive Discussion



based on a parameterized stratospheric transport scheme. The influence of season is a function of seasonal and hemispheric variations in stratospheric dynamics, therefore, the ability to accurately predict the influence of eruption season on volcanic impacts depends on accurate simulation of the dynamics of the stratosphere. Given the rather good agreement between observations and model simulated spatial and size evolution of volcanic aerosols after the 1991 Pinatubo eruption shown in Sect. 3, and prior validation of the underlying MAECHAM5 GCM (e.g., Manzini et al., 2006; Charlton et al., 2007; Thomas et al., 2009a,b), the results shown here suggest that the sensitivity to season of eruption is in reality stronger than suggested by the results of Gao et al. (2008).

In order to address how season of eruption impacts the resulting anomalies in solar shortwave (SW) radiation reaching the surface, we have examined both clear-sky and all-sky SW radiative flux anomalies. Clear-sky SW radiative flux anomalies are a function of the AOD and the seasonal cycle of solar insolation, and as a result, the general features (e.g., peaks, or hemispheric asymmetry) of the clear-sky SW anomalies may not be the same as that of the AOD field. The sensitivity of cumulative SW anomalies to eruption season is generally equal to or weaker than that of the AOD in midlatitudes and in the tropics, but stronger than that of the AOD in the high latitudes due to the strong seasonal cycle in solar insolation at high latitudes. In the global mean, clear-sky SW anomalies are less sensitive to eruption season than AOD, but still significantly greater than zero.

All-sky SW radiative flux anomalies are a function of the clear-sky SW radiative flux anomalies and the model clouds. We found that in the E17 experiment, differences in post-eruption all-sky SW radiative flux anomalies between simulations with eruptions in different seasons were smaller than the natural variability of a control run, meaning that season of eruption would have a insignificant impact on all-sky SW radiative flux anomalies in any one simulation. These model results suggest that clouds are likely as important as season of eruption in determining the total radiative impact of a tropical volcanic eruption with magnitude comparable to Pinatubo.

Influence of season on impact of tropical eruptions

M. Toohey et al.

[Title Page](#)[Abstract](#)[Introduction](#)[Conclusions](#)[References](#)[Tables](#)[Figures](#)[◀](#)[▶](#)[◀](#)[▶](#)[Back](#)[Close](#)[Full Screen / Esc](#)[Printer-friendly Version](#)[Interactive Discussion](#)

**Influence of season
on impact of tropical
eruptions**

M. Toohey et al.

Title Page

Abstract

Introduction

Conclusions

References

Tables

Figures

◀

▶

◀

▶

Back

Close

Full Screen / Esc

Printer-friendly Version

Interactive Discussion



We found that sensitivity to eruption season is different for eruptions of different SO₂ injection magnitudes. Sensitivity of global mean AOD and clear-sky SW anomalies was found to be stronger, in relative terms, for the E17 experiment, with values on the order of 20 %, compared to 12–16 % for the E700 experiment. This can be understood to be related to the fact that cross-equator transport was much more sensitive to season of eruption for the weaker eruption, leading to more variation in hemispheric asymmetry. We plan future sensitivity studies to examine in detail how the hemispheric asymmetry of aerosol transport depends on the magnitude and latitude of eruption, as well as the season. For example, since planetary-wave production and the BDC are generally stronger in the NH, we would not expect the results shown here for an eruption at 15° N to be exactly comparable to an eruption at 15° S.

While the impact of eruption season on all-sky SW anomalies was found to be insignificant for the E17 experiment, for the larger E700 eruption, global mean all-sky SW anomaly sensitivity is significantly greater than zero, and comparable to that of the other fields with a percent sensitivity of 16 %. This result underscores the fact that in order for differences in SW anomalies between different eruption months to be significant compared to the noise induced by clouds, the magnitude of the eruption needs to be quite large.

A larger than previously assumed sensitivity of AOD to eruption season result has implications for reconstructions of past volcanic forcing data sets. It implies that unless season of eruption can be deduced from the proxy records, then the choice of an arbitrary month of eruption can lead to uncertainty in the aerosol evolution. Based on the results of our model simulations, an unknown month of eruption could lead to uncertainties in global mean AOD larger than 20 %, and uncertainties in cumulative zonal mean AOD of greater than 50 % in the mid- to high latitudes.

On the other hand, our model results imply that for Pinatubo-magnitude eruptions, variations in AOD based on season of eruption do not translate into significant differences in all-sky surface shortwave radiative anomalies. This is primarily due to the effects of clouds in the mid- to high latitudes, which greatly reduce the absolute dif-

ference in SW radiation between different eruption seasons, bringing such differences within the range of natural variability. This result implies that using an AOD pattern of arbitrary month of eruption for a Pinatubo-magnitude eruption in a climate model should likely produce no appreciable error in the surface all-sky SW radiation anomalies.

5 At eruption magnitudes larger than Pinatubo, differences in all-sky radiation brought about by differing season of eruption become significant: we found that for a near-super eruption, sensitivity to eruption season was significant for most latitudes, and in the global mean. Global mean all-sky SW anomalies showed a sensitivity to eruption season of approximately 18 %, with eruptions in solstice conditions (January and July)
10 leading to largest anomalies. Thus, for such large eruptions, unknown season of eruption would be an appreciable source of uncertainty in an AOD reconstruction, although the size of this uncertainty is certainly not larger than other uncertainties inherent in estimating AOD timeseries from paleo records (e.g., Robock and Free, 1995).

Some issues need to be considered when interpreting the sensitivity of SW anomalies shown here in terms of possible surface climate effects. Firstly, any changes in cloud fields brought about by the volcanic aerosol through mechanisms not included in the MAECHAM5-HAM could change the surface radiation budget sensitivity to season. For example, post eruption increases in cloud reflectivity due to volcanic aerosols acting as cloud condensation nuclei (Jensen and Toon, 1992) could conceivably affect the sensitivity to eruption season, although many studies (e.g., Wyl, 1999; Luo, Zhengzhao et al., 2002) have reported no significant changes in cloud properties after the Pinatubo eruption. The decrease in sensitivity to eruption season of all-sky SW compared to clear-sky short wave in our Pinatubo-magnitude experiment hints at a possible cloud feedback mechanism, however investigating such a possibility would require
20 a more complex treatment of the interaction between clouds and volcanic aerosols (e.g., Lohmann, 2003). Secondly, it should be kept in mind that radiation anomalies do not necessarily translate directly into temperature anomalies since the thermal inertia of oceans dampens the surface temperature response to radiative anomalies. A full understanding of the surface energy budget should include analysis of latent and
25

Influence of season on impact of tropical eruptions

M. Toohey et al.

[Title Page](#)[Abstract](#)[Introduction](#)[Conclusions](#)[References](#)[Tables](#)[Figures](#)[⏪](#)[⏩](#)[◀](#)[▶](#)[Back](#)[Close](#)[Full Screen / Esc](#)[Printer-friendly Version](#)[Interactive Discussion](#)

sensible heat fluxes, although studies of volcanic impacts with a coupled atmosphere-ocean model have shown these flux anomalies are generally a factor of four smaller than the SW anomalies (Stenchikov et al., 2009).

Finally, it should be pointed out that dynamical responses to volcanic eruptions which can affect surface temperatures, for example the “winter warming phenomenon” (e.g., Robock, 2000), may be more sensitive to season of eruption than radiative fluxes. Comparison of our E17 and E700 simulation results shows that the dynamical effects of large eruptions, which produce significant heating of the tropical lower stratosphere, create much different aerosol transport patterns than weaker eruptions. It is likely that the induced polar vortices have significant effects on surface climate through dynamical coupling of the stratosphere and troposphere (e.g., Stenchikov, 2002). However, volcanic aerosol reconstructions which treat aerosols as passive tracers will not reproduce the type of aerosol evolution shown here. We conclude that in order for climate models with prescribed aerosol forcing to reproduce the most realistic radiative and dynamical perturbations resulting from very large volcanic eruptions, it may be necessary to use aerosol reconstructions which take into account the impact of aerosol heating on stratospheric dynamics.

Acknowledgements. This work has benefited greatly from stimulating discussions within the MPI-M Super Volcano project. This publication is contribution 219 of the Sonderforschungsbereich 574 Volatiles and Fluids in Subduction Zones at Kiel University. U. Niemeier acknowledges funding by the FP7 project IMPLICC. Computations were performed at the German Climate Computer Center (DKRZ).

References

- Ammann, C. M., Meehl, G. A., Washington, W. M., and Zender, C. S.: A monthly and latitudinally varying volcanic forcing dataset in simulations of 20th century climate, *Geophys. Res. Lett.*, 20(12), 1657, doi:10.1029/2003GL016875, 2003. 22445
- Barkstrom, B. R.: The Earth Radiation Budget Experiment (ERBE), *Am. Meteorol. Soc.*, 1170–1185, 1984. 22451

Influence of season on impact of tropical eruptions

M. Toohey et al.

Title Page

Abstract

Introduction

Conclusions

References

Tables

Figures



Back

Close

Full Screen / Esc

Printer-friendly Version

Interactive Discussion



Influence of season on impact of tropical eruptions

M. Toohey et al.

Title Page

Abstract

Introduction

Conclusions

References

Tables

Figures

◀

▶

◀

▶

Back

Close

Full Screen / Esc

Printer-friendly Version

Interactive Discussion



- Barkstrom, B. R. and Smith, G. L.: The Earth Radiation Budget Experiment: Science and implementation, *Rev. Geophys.*, p. 379, doi:10.1029/RG024i002p00379, 22451
- Bender, F. A.-M., Ekman, A. M. L., and Rodhe, H.: Response to the eruption of Mount Pinatubo in relation to climate sensitivity in the CMIP3 models, *Clim. Dynam.*, 35, 875–886, doi:10.1007/s00382-010-0777-3, 2010. 22457
- Charlton, A. J., Polvani, L. M., Perlwitz, J., Sassi, F., Manzini, E., Shibata, K., Pawson, S., Nielsen, J. E., and Rind, D.: A New Look at Stratospheric Sudden Warmings. Part II: Evaluation of Numerical Model Simulations, *J. Climate*, 470–488, doi:10.1175/JCLI3994.1. 22462
- Charney, J. G. and Drazin, P. G.: Propagation of Planetary-Scale Disturbances from the Lower into the Upper Atmosphere, *J. Geophys. Res.*, 66, 83–109, doi:10.1029/JZ066i001p00083, 1961. 22445
- Fouquart, Y. and Bonnel, B.: Computations of solar heating of the earth's atmosphere: A new parameterization, *Contrib. Atmos. Phys.*, 53, 35–62, 1980. 22448
- Gao, C., Robock, A., and Ammann, C.: Volcanic forcing of climate over the past 1500 years: An improved ice core-based index for climate models, *J. Geophys. Res. Atmos.*, 113, 23111, doi:10.1029/2008JD010239, 2008. 22446, 22461, 22462
- Giorgetta, M. A., Manzini, E., Roeckner, E., Esch, M., and Bengtsson, L.: Climatology and Forcing of the Quasi-Biennial Oscillation in the MAECHAM5 Model, *J. Clim.*, 19, 3882, doi:10.1175/JCLI3830.1, 2006. 22447
- Guo, S.: Re-evaluation of SO₂ release of the 15 June 1991 Pinatubo eruption using ultraviolet and infrared satellite sensors, *Geochem. Geophys. Geosyst.*, 5(4), Q04001, doi:10.1029/2003GC000654, 2004a. 22447
- Guo, S.: Particles in the great Pinatubo volcanic cloud of June 1991: The role of ice, *Geochem. Geophys. Geosyst.*, 5(5), Q05003, doi:10.1029/2003GC000655, 2004b. 22448
- Hamill, P., Jensen, E. J., Russell, P. B., and Bauman, J. J.: The Life Cycle of Stratospheric Aerosol Particles, *B. Am. Meteorol. Soc.*, 78(7), 1395–1410, doi:10.1175/1520-0477(1997)078<1395:TLCOSA>2.0.CO;2, 1997. 22445
- Holton, J. R., Haynes, P. H., McIntyre, M. E., Douglass, A. R., Rood, R. B., and Pfister, L.: Stratosphere-Troposphere Exchange, *Rev. Geophys.*, 33, 403–439, doi:10.1029/95RG02097, 1995. 22445
- Jensen, E. J. and Toon, O. B.: The potential effects of volcanic aerosols on cirrus cloud microphysics, *Geophys. Res. Lett.*, 19, 1759, doi:10.1029/92GL01936, 1992. 22464
- Kirchner, I., Stenchikov, G. L., Graf, H.-F., Robock, A., and Antuña, J. C.: Climate model sim-

Influence of season on impact of tropical eruptions

M. Toohey et al.

Title Page

Abstract

Introduction

Conclusions

References

Tables

Figures

◀

▶

◀

▶

Back

Close

Full Screen / Esc

Printer-friendly Version

Interactive Discussion



ulation of winter warming and summer cooling following the 1991 Mount Pinatubo volcanic eruption, *J. Geophys. Res.*, 19039–19055, doi:10.1029/1999JD900213, 1999. 22457

Kodera, K.: Influence of volcanic eruptions on the troposphere through stratospheric dynamical processes in the northern hemisphere winter, *J. Geophys. Res.*, 1273–1282, doi:10.1029/93JD02731, 1994. 22457

Kodera, K. and Kuroda, Y.: Tropospheric and stratospheric aspects of the Arctic oscillation, *Geophys. Res. Lett.*, 27(20), p. 3349, doi:10.1029/2000GL012017, 2000a. 22457

Kodera, K. and Kuroda, Y.: A mechanistic model study of slowly propagating coupled stratosphere-troposphere variability, *J. Geophys. Res.*, 105(D10), 12361–12370, doi:10.1029/2000JD900094, 2000b. 22457

Kokkola, H., Hommel, R., Kazil, J., Niemeier, U., Partanen, A.-I., Feichter, J., and Timmreck, C.: Aerosol microphysics modules in the framework of the ECHAM5 climate model – intercomparison under stratospheric conditions, *Geosci. Model Dev.*, 2, 97–112, doi:10.5194/gmd-2-97-2009, 2009. 22448

Kravitz, B. and Robock, A.: Climate effects of high-latitude volcanic eruptions: Role of the time of year, *J. Geophys. Res.*, 116, D01105, doi:10.1029/2010JD014448, <http://www.agu.org/pubs/crossref/2011/2010JD014448.shtml>, 2011. 22446

Kutterolf, S., Freundt, A., and Peréz, W.: Pacific offshore record of plinian arc volcanism in Central America: 2. Tephra volumes and erupted masses, *Geochem., Geophys. Geosyst.*, 9(2), Q02S02, doi:10.1029/2007GC001791, 2008a. 22449

Kutterolf, S., Freundt, A., Peréz, W., Mörz, T., Schacht, U., Wehrmann, H., and Schmincke, H.: Pacific offshore record of plinian arc volcanism in Central America: 1. Along-arc correlations, *Geochem. Geophys. Geosyst.*, 9(2), Q02S01, doi:10.1029/2007GC001631, 2008b. 22449

Labitzke, K. and McCormick, M. P.: Stratospheric temperature increases due to Pinatubo aerosols, *Geophys. Res. Lett.*, 19, 207–210, doi:10.1029/91GL02940, 1992. 22457

Lin, S.-J. and Rood, R. B.: Multidimensional Flux-Form Semi-Lagrangian Transport Schemes, *Mon. Weather Rev.*, 124(9), 2046–2070, doi:10.1175/1520-0493(1996)124<2046:MFFSLT>2.0.CO;2, 1996. 22448

Lohmann, U.: Impact of the Mount Pinatubo eruption on cirrus clouds formed by homogeneous freezing in the ECHAM4 GCM, *J. Geophys. Res.*, 108(D18), 4568, doi:10.1029/2002JD003185, 2003. 22464

Luo, Zhengzhao, Rossow, William B., Inoue, Toshiro, and Stubenrauch, Claudia J.: Did the Eruption of the Mt. Pinatubo Volcano Affect Cirrus Properties?., *J. Clim.*, 15(19), 2806–2820,

Influence of season on impact of tropical eruptions

M. Toohey et al.

Title Page

Abstract

Introduction

Conclusions

References

Tables

Figures

◀

▶

◀

▶

Back

Close

Full Screen / Esc

Printer-friendly Version

Interactive Discussion



doi:10.1175/1520-0442(2002)015<2806:DTEOTM>2.0.CO;2, 2002. 22464

Manzini, E., Giorgetta, M. A., Esch, M., Kornblueh, L., and Roeckner, E.: The Influence of Sea Surface Temperatures on the Northern Winter Stratosphere: Ensemble Simulations with the MAECHAM5 Model, *J. Clim.*, 3863–3881, doi:10.1175/JCLI3826.1. 22462

5 McIntyre, M. E. and Palmer, T. N.: Breaking planetary waves in the stratosphere, *Nature*, 305, 593–600, doi:10.1038/305593a0, 1983. 22445

Mlawer, E. J., Taubman, S. J., Brown, P. D., Iacono, M. J., and Clough, S. A.: Radiative transfer for inhomogeneous atmospheres: RRTM, a validated correlated-k model for the longwave, *J. Geophys. Res.*, 102(D14), 16663–16682, doi:10.1029/97JD00237. 22448

10 Niemeier, U., Timmreck, C., Graf, H., Kinne, S., Rast, S., and Self, S.: Initial fate of fine ash and sulfur from large volcanic eruptions, *Atmos. Chem. Phys.*, 9, 9043–9057, doi:10.5194/acp-9-9043-2009, 2009. 22447, 22448, 22450, 22451

Niemeier, U., Schmidt, H., and Timmreck, C.: The dependency of geoengineered sulfate aerosol on the emission strategy, *Atmos. Sci. Lett.*, 12(2), 189–194, doi:10.1002/asl.304, 2010. 22455

15 Perlwitz, J. and Graf, H.-F.: The Statistical Connection between Tropospheric and Stratospheric Circulation of the Northern Hemisphere in Winter, *J. Climate*, 12(2), 189–194, doi:10.1175/1520-0442(1995)008<2281:TSCBTA>2.0.CO;2. 22457

Randel, W. J., Garcia, R. R., and Wu, F.: Time-Dependent Upwelling in the Tropical Lower Stratosphere Estimated from the Zonal-Mean Momentum Budget, *J. Atmos. Sci.*, 59, 2141–2152, doi:10.1175/1520-0469(2002)059<2141:TDUITT>2.0.CO;2, 2002. 22455

20 Read, W. G., Froidevaux, L., and Waters, J. W.: Microwave limb sounder measurement of stratospheric SO₂ from the Mt. Pinatubo Volcano, *Geophys. Res. Lett.*, 20, 1299, doi:10.1029/93GL00831, 1993. 22448

25 Robock, A.: Volcanic eruptions and climate, *Rev. Geophys.*, 38, 191–220, doi:10.1029/1998RG000054, 2000. 22445, 22465

Robock, A. and Free, M. P.: Ice cores as an index of global volcanism from 1850 to the present, *J. Geophys. Res.*, 100, 11549–11568, doi:10.1029/95JD00825, 1995. 22464

30 Roeckner, E., Baeuml, G., Bonaventura, L., Brokopf, R., Esch, M., Giorgetta, M., Hagemann, S., Kirchner, I., Kornblueh, L., Manzini, E., Rhodin, A., Schlese, U., Schulzweida, U., and Tompkins, A.: The atmospheric general circulation model ECHAM5 – Part I, Tech. rep., MPI Report No. 349, 2003. 22448

Rose, W., Newhall, C., Bornhorst, T., and Self, S.: Quaternary silicic pyroclastic deposits of

Influence of season on impact of tropical eruptions

M. Toohey et al.

Title Page

Abstract

Introduction

Conclusions

References

Tables

Figures

◀

▶

◀

▶

Back

Close

Full Screen / Esc

Printer-friendly Version

Interactive Discussion



Atitlán Caldera, Guatemala, *J. Volcanol. Geotherm. Res.*, 33, 57–80, doi:10.1016/0377-0273(87)90054-0, 1987. 22449

Rosenlof, K. H.: Seasonal cycle of the residual mean meridional circulation in the stratosphere, *J. Geophys. Res.*, 100, 5173–5191, doi:10.1029/94JD03122, 1995. 22445

5 Russell, P. B., Livingston, J. M., Pueschel, R. F., Bauman, J. J., Pollack, J. B., Brooks, S. L., Hamill, P., Thomason, L. W., Stowe, L. L., Deshler, T., Dutton, E. G., and Bergstrom, R. W.: Global to microscale evolution of the Pinatubo volcanic aerosol derived from diverse measurements and analyses, *J. Geophys. Res.*, 101, 18745–18763, doi:10.1029/96JD01162, 1996. 22450

10 Sato, M., Hansen, J. E., McCormick, M. P., and Pollack, J. B.: Stratospheric Aerosol Optical Depths, 1850–1990, *J. Geophys. Res.*, 98, 22987–22994, doi:10.1029/93JD02553, 1993. 22451, 22460, 22471

Schmincke, H.-U.: *Volcanism*, Springer-Verlag, Heidelberg, Germany, p. 267, 2004. 22449

15 Schoeberl, M. R. and Hartmann, D. L.: The dynamics of the stratospheric polar vortex and its relation to springtime ozone depletions, *Science (New York, NY)*, 251, 46–52, doi:10.1126/science.251.4989.46, 1991. 22458

Self, S.: The effects and consequences of very large explosive volcanic eruptions., *Philosophical transactions, Series A, Math. Phys. Eng. Sci.*, 364, 1845, 2073–2097, doi:10.1098/rsta.2006.1814, 2006. 22447

20 Shindell, D. T., Schmidt, G. A., Miller, R. L., and Rind, D.: Northern Hemisphere winter climate response to greenhouse gas, ozone, solar, and volcanic forcing, *J. Geophys. Res.*, 7193–7210, doi:10.1029/2000JD900547, 2001. 22457

Stenchikov, G.: Arctic Oscillation response to the 1991 Mount Pinatubo eruption: Effects of volcanic aerosols and ozone depletion, *Journal of Geophysical Research*, 107, doi:10.1029/2002JD002090, 2002. 22465

25 Stenchikov, G., Delworth, T. L., Ramaswamy, V., Stouffer, R. J., Wittenberg, A., and Zeng, F.: Volcanic signals in oceans, *J. Geophys. Res.*, 114, D16104, doi:10.1029/2008JD011673, 2009. 22465

30 Stenchikov, G. L., Kirchner, I., Robock, A., Graf, H., Antuña, J. C., Grainger, R. G., Lambert, A., and Thomason, L.: Radiative forcing from the 1991 Mount Pinatubo volcanic eruption, *J. Geophys. Res.*, 103, 13837–13858, doi:10.1029/98JD00693, 1998. 22452

Stier, P., Feichter, J., Kinne, S., Kloster, S., Vignati, E., Wilson, J., Ganzeveld, L., Tegen, I., Werner, M., Balkanski, Y., Schulz, M., Boucher, O., Minikin, A., and Petzold, A.: The aerosol-

climate model ECHAM5-HAM, *Atmos. Chem. Phys.*, 5, 1125–1156, doi:10.5194/acp-5-1125-2005, 2005. 22448

Thomas, M. A., Giorgetta, M. A., Timmreck, C., Graf, H.-F., and Stenchikov, G.: Simulation of the climate impact of Mt. Pinatubo eruption using ECHAM5 – Part 2: Sensitivity to the phase of the QBO and ENSO, *Atmos. Chem. Phys.*, 9, 3001–3009, doi:10.5194/acp-9-3001-2009, 2009a. 22462

Thomas, M. A., Timmreck, C., Giorgetta, M. A., Graf, H.-F., and Stenchikov, G.: Simulation of the climate impact of Mt. Pinatubo eruption using ECHAM5 – Part 1: Sensitivity to the modes of atmospheric circulation and boundary conditions, *Atmos. Chem. Phys.*, 9, 757–769, doi:10.5194/acp-9-757-2009, 2009b. 22462

Timmreck, C., Graf, H.-F., and Kirchner, I.: A one and half year interactive MA/ECHAM4 simulation of Mount Pinatubo Aerosol, *J. Geophys. Res.*, 104, 9337–9359, doi:10.1029/1999JD900088, 1999. 22449

Trepte, C. R. and Hitchman, M. H.: Tropical stratospheric circulation deduced from satellite aerosol data, *Nature*, 355, 626–628, doi:10.1038/355626a0, 1992. 22461

Vignati, E.: M7: An efficient size-resolved aerosol microphysics module for large-scale aerosol transport models, *J. Geophys. Res.*, 109, D22202, doi:10.1029/2003JD004485, 2004. 22448

Waugh, D. W.: Seasonal variation of isentropic transport out of the tropical stratosphere, *J. Geophys. Res.*, 101, 4007–4023, doi:10.1029/95JD03160, 1996. 22445

Wielicki, B. A., Wong, T., Allan, R. P., Slingo, A., Kiehl, J. T., Soden, B. J., Gordon, C. T., Miller, A. J., Yang, S.-K., Randall, D. A., Robertson, F., Susskind, J., and Jacobowitz, H.: Evidence for large decadal variability in the tropical mean radiative energy budget., *Science (New York, N.Y.)*, 841–844, doi:10.1126/science.1065837, 2002. 22451

Wong, T., Wielicki, B. A., Lee, R. B., Smith, G. L., Bush, K. A., and Willis, J. K.: Reexamination of the Observed Decadal Variability of the Earth Radiation Budget Using Altitude-Corrected ERBE/ERBS Nonscanner WFOV Data, *J. Clim.*, 4028–4040, doi:10.1175/JCLI3838.1, 2006. 22451

Wylie, D. P. and Menzel, W. P.: , Eight Years of High Cloud Statistics Using HIRS, *J. Climate*, 1(12), 170–184, 1999. 22464

Young, R. E., Houben, H., and Toon, O. B.: Radiatively forced dispersion of the Mt. Pinatubo volcanic cloud and induced temperature perturbations in the stratosphere during the first few months following the eruption, *Geophys. Res. Lett.*, p. 369, doi:10.1029/93GL03302, 1994. 22449

Influence of season on impact of tropical eruptions

M. Toohey et al.

Title Page

Abstract

Introduction

Conclusions

References

Tables

Figures

◀

▶

◀

▶

Back

Close

Full Screen / Esc

Printer-friendly Version

Interactive Discussion



Influence of season on impact of tropical eruptions

M. Toohey et al.

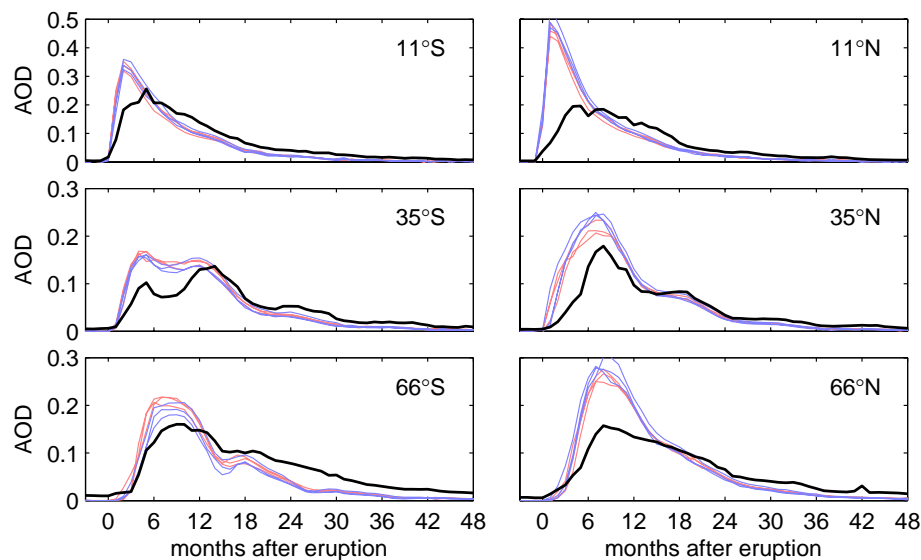


Fig. 1. Monthly-mean, zonal-mean $0.55\ \mu\text{m}$ AOD at labelled latitudes, from Pinatubo eruption period observations of the Sato et al. (1993) timeseries (black) and MAECHAM5-HAM Pinatubo-magnitude eruption simulations with eruptions at $15^\circ\ \text{N}$, $91^\circ\ \text{W}$ (red) and $15^\circ\ \text{N}$, $120^\circ\ \text{E}$ (blue).

[Title Page](#)[Abstract](#)[Introduction](#)[Conclusions](#)[References](#)[Tables](#)[Figures](#)[◀](#)[▶](#)[◀](#)[▶](#)[Back](#)[Close](#)[Full Screen / Esc](#)[Printer-friendly Version](#)[Interactive Discussion](#)

Influence of season on impact of tropical eruptions

M. Toohey et al.

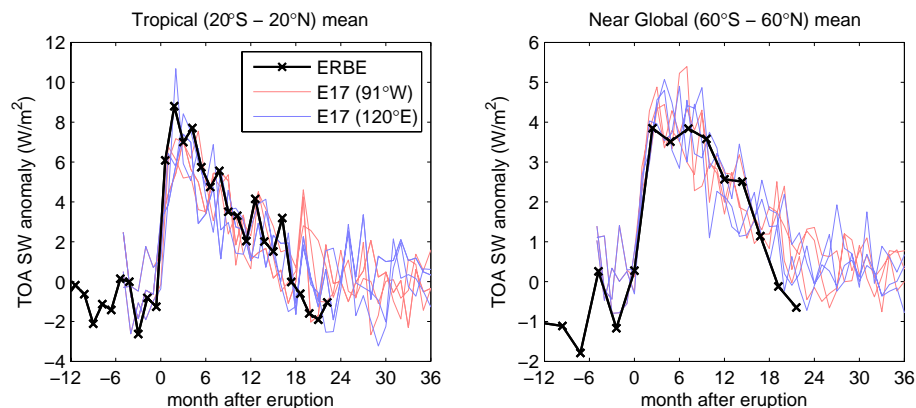


Fig. 2. Tropical (20°S – 20°N) and near-global (60°S – 60°N) reflected shortwave flux anomalies at the top of the atmosphere from Pinatubo eruption period ERBE observations (black) and MAECHAM5-HAM Pinatubo-magnitude eruption simulations with eruptions at 15°N , 91°W (red) and 15°N , 120°E (blue). Model anomalies calculated with respect to a 20-yr control simulation, ERBE anomalies calculated with respect to the 1985–1989 mean.

[Title Page](#)
[Abstract](#)
[Introduction](#)
[Conclusions](#)
[References](#)
[Tables](#)
[Figures](#)
[◀](#)
[▶](#)
[◀](#)
[▶](#)
[Back](#)
[Close](#)
[Full Screen / Esc](#)
[Printer-friendly Version](#)
[Interactive Discussion](#)

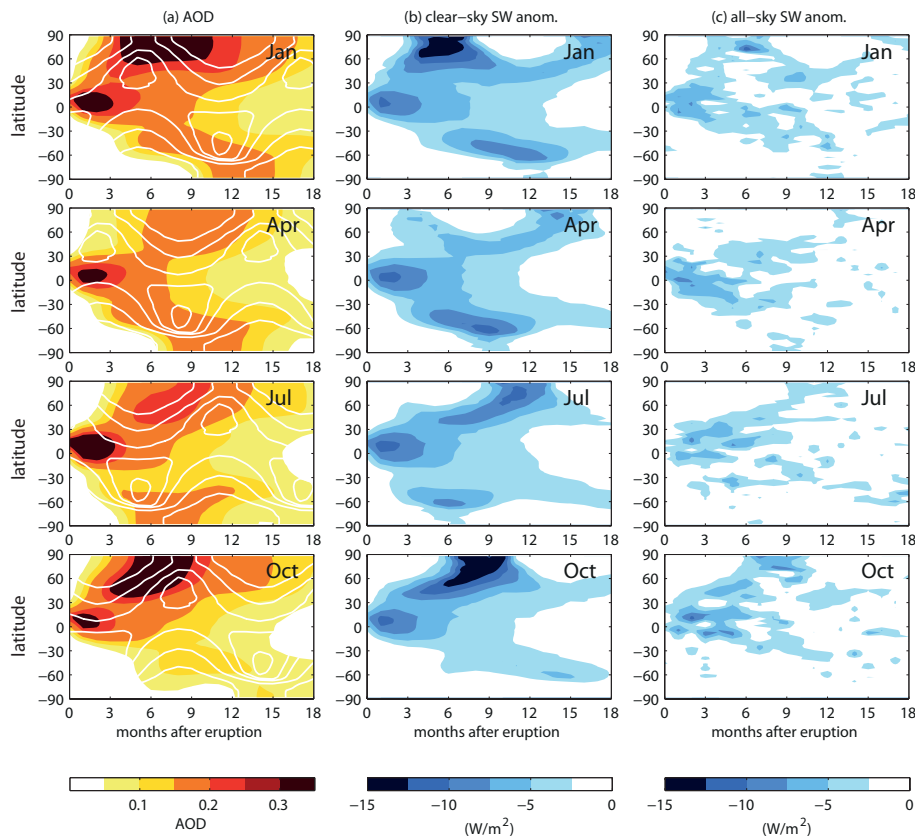



Fig. 3. Zonal mean, monthly mean $0.55\ \mu\text{m}$ aerosol optical depth **(a)**, clear-sky surface shortwave radiation anomalies **(b)** and all-sky surface shortwave anomalies **(c)** for E17 eruptions in January, April, July and October. White contours in column **(a)** show climatological surface clear-sky shortwave radiation. All anomalies shown are ensemble mean differences from a control run, and are significant at the 95 % confidence level.

Influence of season on impact of tropical eruptions

M. Toohey et al.

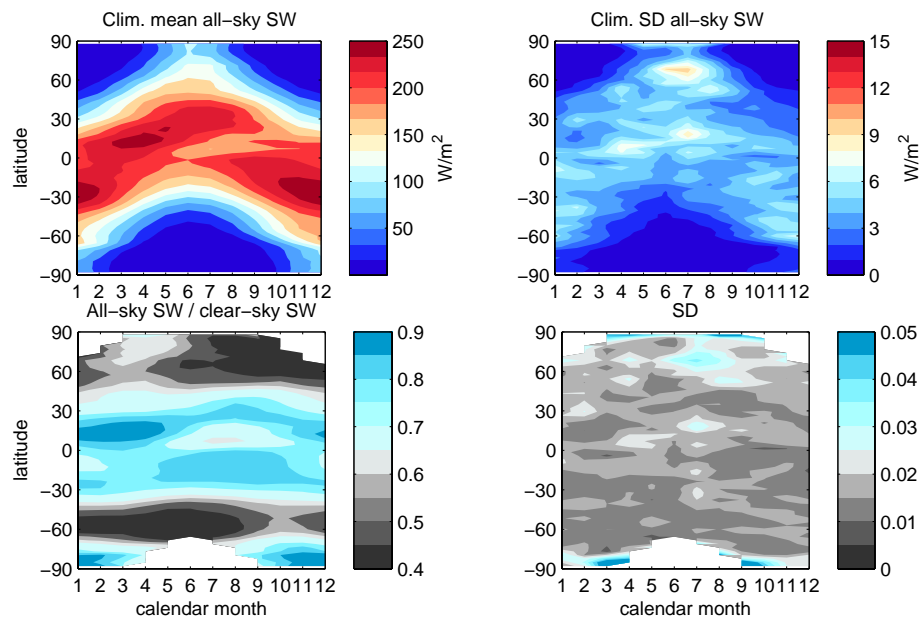


Fig. 4. MAECHAM5-HAM climatological mean values of all-sky SW surface radiation (top) and ratio of all-sky to clear-sky SW surface radiation (bottom) along with the standard deviation (SD) of each field.

[Title Page](#)
[Abstract](#)
[Introduction](#)
[Conclusions](#)
[References](#)
[Tables](#)
[Figures](#)
[Back](#)
[Close](#)
[Full Screen / Esc](#)
[Printer-friendly Version](#)
[Interactive Discussion](#)

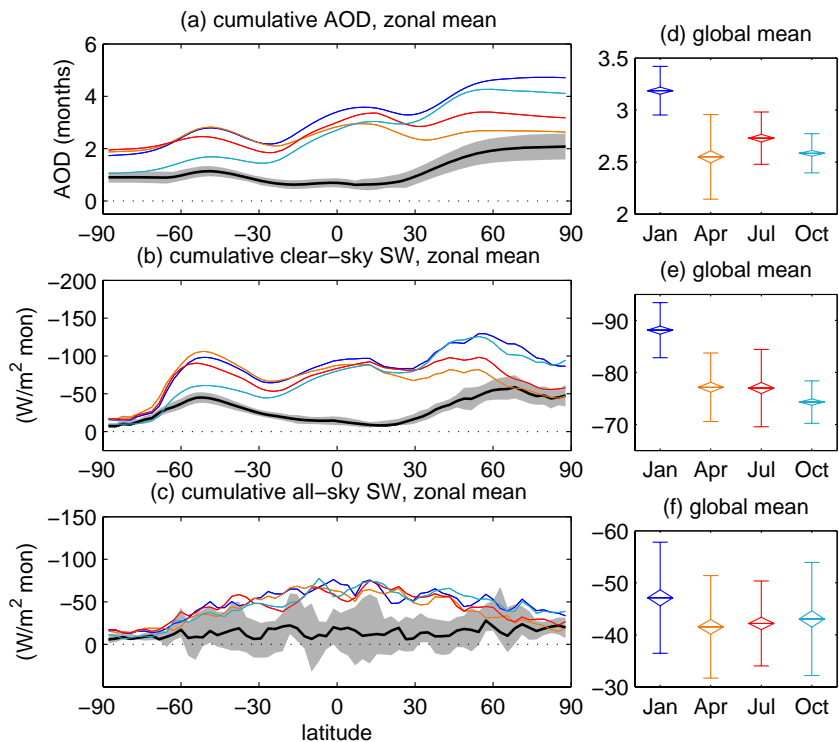


Fig. 5. Zonal mean (left) and global mean (right), two-year-cumulative post-eruption anomalies in AOD (top), clear-sky surface shortwave radiation anomalies (middle) and all-sky surface shortwave anomalies (bottom) for the E17 experiment. Eruption seasons indicated by colors. Black lines in zonal mean plots show mean difference between maximum and minimum response at each latitude, with shading indicating 95 % confidence interval of difference based on the student's t-test. In global mean plots, horizontal lines within diamonds indicates ensemble mean, vertical range of diamonds indicates standard error of mean, and vertical error bars indicate 2σ ensemble variability.

**Influence of season
on impact of tropical
eruptions**

M. Toohy et al.

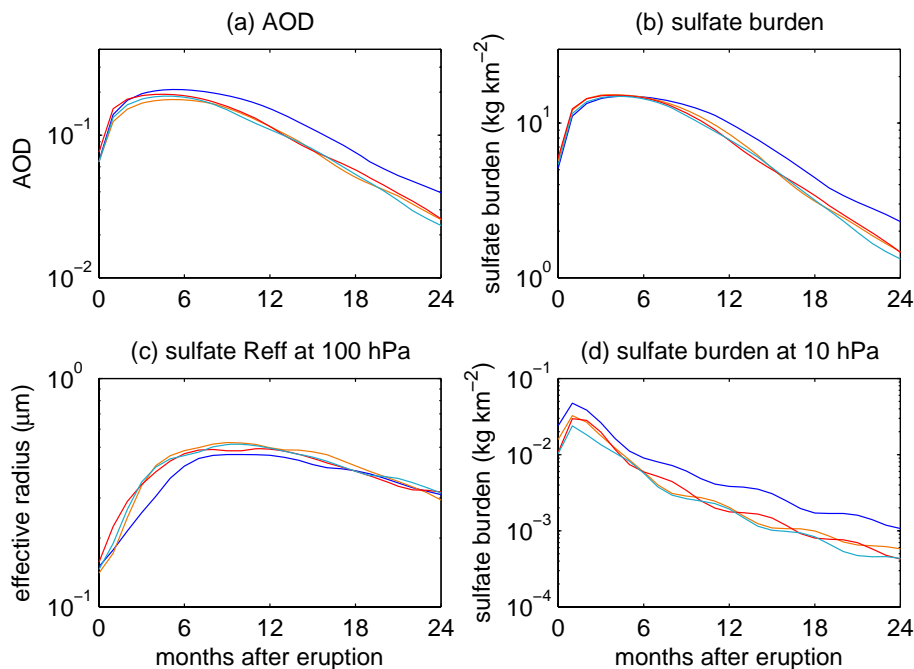


Fig. 6. Timeseries of global mean **(a)** AOD, **(b)** sulfate mass burden, **(c)** sulfate aerosol effective radius at 100 hPa, and **(d)** sulfate mass burden at 10 hPa, for eruptions in January (blue), April (orange), July (red) and October (cyan).

[Title Page](#)[Abstract](#)[Introduction](#)[Conclusions](#)[References](#)[Tables](#)[Figures](#)[◀](#)[▶](#)[◀](#)[▶](#)[Back](#)[Close](#)[Full Screen / Esc](#)[Printer-friendly Version](#)[Interactive Discussion](#)

Influence of season on impact of tropical eruptions

M. Toohey et al.

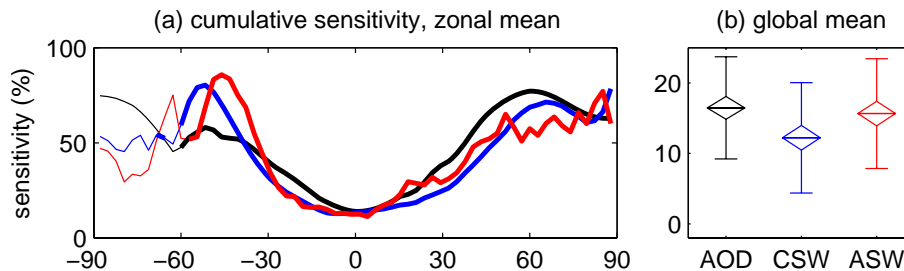


Fig. 7. Percent sensitivity to eruption season for cumulative anomalies of AOD (black), clear-sky surface shortwave radiation (blue) and all-sky surface shortwave radiation (red), calculated as difference between maximum and minimum response (black lines in Fig. 5) divided by minimum response. Zonal mean quantities plotted versus latitude to left **(a)**, global mean quantities plotted in contracted y-scale to right **(b)**. Thick lines in panel a show where response is significant at the 95 % level. In panel **(b)**, horizontal lines within diamonds indicates ensemble mean, vertical range of diamonds indicates standard error of mean, and vertical error bars indicate 2σ ensemble variability.

Title Page

Abstract

Introduction

Conclusions

References

Tables

Figures

◀

▶

◀

▶

Back

Close

Full Screen / Esc

Printer-friendly Version

Interactive Discussion



Influence of season on impact of tropical eruptions

M. Toohey et al.

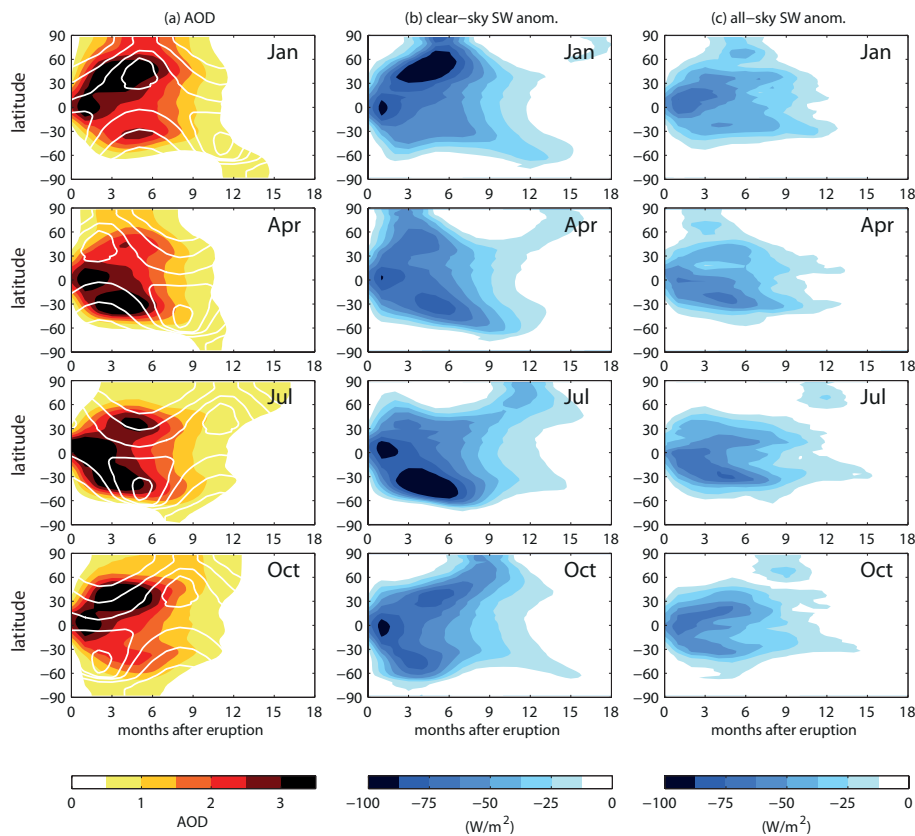


Fig. 8. As Fig. 3, for the E700 experiment.

Title Page

Abstract

Introduction

Conclusions

References

Tables

Figures

◀

▶

◀

▶

Back

Close

Full Screen / Esc

Printer-friendly Version

Interactive Discussion



Influence of season on impact of tropical eruptions

M. Toohey et al.

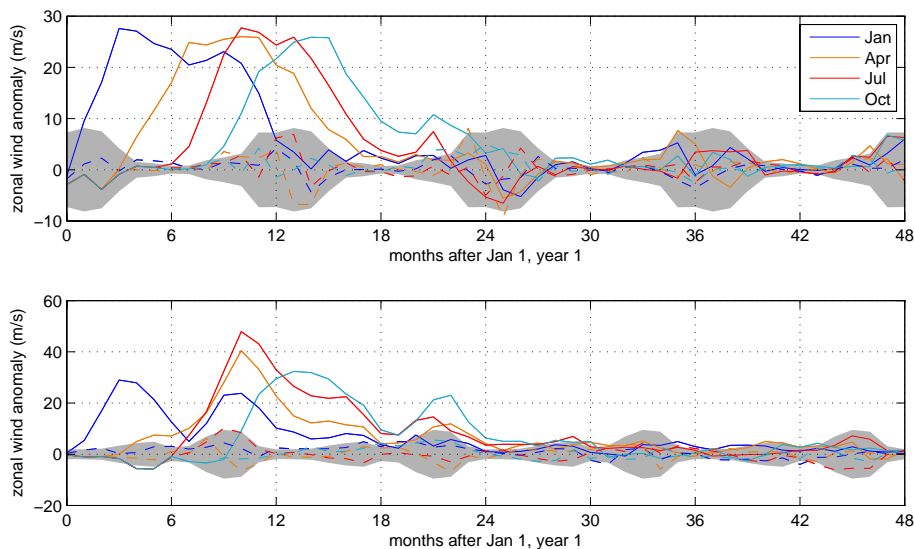


Fig. 9. Zonal mean zonal wind anomalies at 50 hPa and 60° N (top) and 60° S (bottom). Anomalies outside the gray shading are significant at the 95% confidence level based on the variability of a control run. Note different scales for the NH and SH plots.

[Title Page](#)[Abstract](#)[Introduction](#)[Conclusions](#)[References](#)[Tables](#)[Figures](#)[◀](#)[▶](#)[◀](#)[▶](#)[Back](#)[Close](#)[Full Screen / Esc](#)[Printer-friendly Version](#)[Interactive Discussion](#)

Influence of season on impact of tropical eruptions

M. Toohey et al.

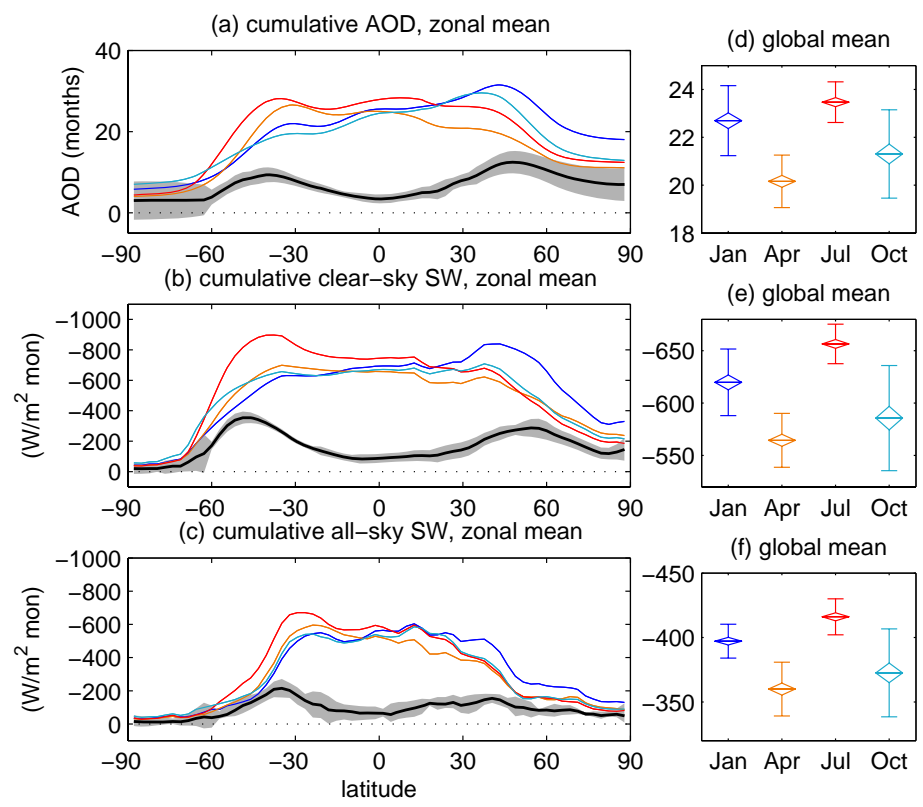


Fig. 10. As Fig. 5, for the E700 experiment. Note different y-axes.

Title Page

Abstract Introduction

Conclusions References

Tables Figures

◀ ▶

◀ ▶

Back Close

Full Screen / Esc

Printer-friendly Version

Interactive Discussion



Influence of season on impact of tropical eruptions

M. Toohey et al.

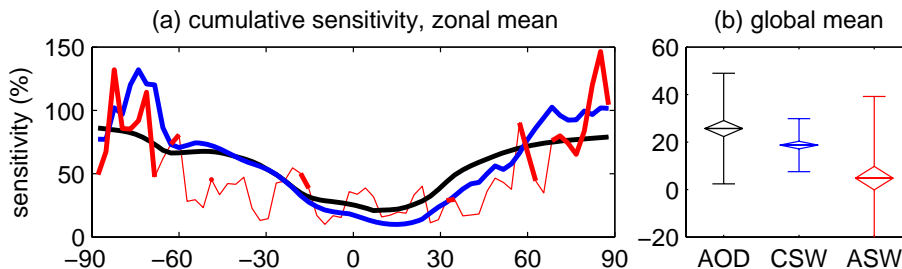


Fig. 11. As Fig. 7, for the E700 experiment. Note different y-axes.

Title Page

Abstract

Introduction

Conclusions

References

Tables

Figures

◀

▶

◀

▶

Back

Close

Full Screen / Esc

Printer-friendly Version

Interactive Discussion

